—研究論文—
Scientific Paper

Simultaneous observations of noctilucent clouds and polar mesosphere summer echoes at Syowa Station, Antarctica

Keisuke Hosokawa[1*], Yasuo Takeda[2], Tadahiko Ogawa[3], Akira Kadokura[4, 5], Akira Sessai Yukimatu[4, 5] and Natsuo Sato[4]

南極昭和基地における NLC と PMSE の同時観測

細川敬祐[1*]・武田康男[2]・小川忠彦[3]・門倉　昭[4, 5]・行松　彰[4, 5]・佐藤夏雄[4]

(Received December 11 2012; Accepted March 8, 2013)

要旨: 昭和基地における夜光雲（NLC）と極域夏季中間圏レーダーエコー（PMSE）の同時観測について報告する．2009 年 2 月 11 日の 2000 UT から 2130 UT の間，昭和基地の南側において夜光雲が目視観測された．同時に，昭和基地 SuperDARN 短波レーダーが近距離レンジにおいて特徴的なエコーを観測した．このエコーは小さいドップラー速度とスペクトル幅を持ち，短波レーダーによって観測される PMSE の特徴と調和的であるが，同じ時間帯に NLC が観測されたことから，この特徴的な近距離エコーが PMSE であることが確認された．これに加え，NLC と PMSE の空間分布は良い一致を示し，これは短波レーダーによる観測が PMSE や NLC の 2 次元分布を知る上で有用なツールになることを示唆するものである．

Abstract: This paper reports simultaneous observations of visible noctilucent clouds (NLC) and polar mesosphere summer echoes (PMSE) at Syowa Station (69°01′S, 38°61′E) in Antarctica. During a 1.5 h interval from 2000 to 2130 UT (2300 to 0030 LT) on Feb. 11, 2009, visible NLC were observed south of Syowa Station. The oblique sounding HF radar of SuperDARN at Syowa Station simultaneously observed peculiar echoes in the closest two range gates. The echoes had a small Doppler velocity and a narrow spectral width, which are consistent with the characteristics of PMSE in the SuperDARN data. The simultaneous appearance of the visible NLC and peculiar near-range echoes observed by the HF radar suggests that the echoes were actually a signature of PMSE in the HF band. In addition, the data from the simultaneous measurements show that the spatial distributions of NLC and PMSE in the HF band were collocated with each other, which

[1] 電気通信大学大学院情報理工学研究科．Graduate School of Informatics and Engineering, University of Electro-Communications, Chofugaoka 1–5–1, Chofu, Tokyo 182-8585.
[2] 第 50 次日本南極地域観測隊．50th Japanese Antarctic Research Expedition.
[3] 情報通信研究機構．National Institute of Information and Communications Technology, Nukui-kitamachi 4–2–1, Koganei, Tokyo 184-8795.
[4] 情報・システム研究機構国立極地研究所．National Institute of Polar Research, Research Organization of Information and Systems, Midori-cho 10–3, Tachikawa, Tokyo 190-8518.
[5] 総合研究大学院大学複合科学研究科極域科学専攻．Department of Polar Science, School of Multidisciplinary Sciences, The Graduate University for Advanced Studies (SOKENDAI), Midori-cho 10–3, Tachikawa, Tokyo 190-8518.
* Corresponding author. E-mail: keisuke.hosokawa@uec.ac.jp

南極資料，Vol. 57，No. 3，317–328，2013
Nankyoku Shiryô (Antarctic Record), Vol. 57, No. 3, 317–328, 2013

implies that oblique sounding HF radar is a useful tool for estimating the two-dimensional horizontal distribution of PMSE.

1. Introduction

The polar summer mesosphere has attracted increasing interest in recent years. The temperature at the summer solstice is known to be much colder than that expected from radiative equilibrium, which is presumably due to the effect of pole to pole meridional circulation driven by gravity waves (*e.g.*, McIntyre, 1989). Temperature measurements made by rocket experiments have shown that the summer polar mesosphere is the coldest region on the Earth (*e.g.*, Lübken and von Zahn, 1991). The cold temperature results in the formation of ice particles in the mesosphere, which are visible from the ground as noctilucent clouds (NLC), also termed polar mesospheric clouds (PMC). Polar mesosphere summer echoes (PMSE) are also important features associated with the cold polar summer mesosphere. PMSE are strong radar echoes scattered from Bragg-scale structures within the plasma and neutral gases in the summer polar mesosphere (Cho and Röttger, 1997; Rapp and Lübken, 2004), which have been observed with VHF radars in the Northern Hemisphere (NH). It has been established that PMSE are closely associated with an existence of small ice particles, some of which can be detected optically as NLC. PMSE can therefore be considered to be manifestations of NLC in radar observations. The mean altitude of NLC is about 84 km, whereas that of PMSE is about 85.3 km (Klekociuk *et al.*, 2008).

Recently, progress in the study of PMSE has been made from observations in the Southern Hemisphere (SH). The first clear observation was made with a 50 MHz radar in 1994 by Woodman *et al.* (1999), who showed that the echoes in the SH were much weaker than those in the NH. Several groups then detected Antarctic PMSE in HF (Ogawa *et al.*, 2002; Hosokawa *et al.*, 2004) and VHF (Morris *et al.*, 2004; Lübken *et al.*, 2004) bands. In particular, Ogawa *et al.* (2002) first observed PMSE with the oblique sounding HF radars of Super Dual Auroral Radar Network (SuperDARN) in Antarctica, which enabled an estimation of the global distribution of PMSE in both hemispheres to be made (see also Ogawa *et al.*, 2003). By using the data from the SuperDARN radars in both hemispheres, Hosokawa *et al.* (2005) compared the probability of occurrence of Arctic and Antarctic PMSE. They discovered that the rate of occurrence of Arctic PMSE was 1.5 times higher than that of Antarctic PMSE, which implied a possible interhemispheric asymmetry in the mesospheric temperature. More recently, Latteck *et al.* (2007) used data from well-calibrated VHF radars in both hemispheres and demonstrated that PMSE occurred less frequently in the SH.

As mentioned above, PMSE are manifestations of NLC in radar observations. The relationship between NLC and PMSE has previously been investigated exclusively in the NH (*e.g.*, Nussbaumer *et al.*, 1996). Most of these studies employed lidar and VHF radar of vertical incidence for observing NLC and PMSE, respectively. Hence, the two-dimensional (2-D) horizontal extent of these two structures has not been compared in detail. Recently, Taylor *et al.* (2009) first reported common volume 2-D observations of PMSE and NLC. They used the Poker Flat Incoherent Scatter Radar (PFISR) in Alaska and closely located optical instruments to observe the 2-D structures of PMSE and NLC, and demonstrated

striking similarities in the location and orientation of these two structures in the mesosphere. The first SH common-volume measurements of NLC and PMSE were made by Klekociuk *et al.* (2008), who used Rayleigh lidar and VHF/MST radar at the Australian Davis Antarctic Station to detect NLC and PMSE, respectively. They observed PMSE during 70% of the NLC events in their lidar observations. However, the 2-D spatial relationship between PMSE and NLC was not investigated because their simultaneous observations at Davis were based on measurements made by vertical sounding systems.

In this short report, we present the first simultaneous 2-D observations of visible NLC and PMSE in Antarctica. The observations were made at Syowa Station in Antarctica (69° 01′S, 38°61′E) on Feb. 11, 2009, using high-resolution digital camera imaging and the two oblique sounding HF radars of SuperDARN routinely operated at Syowa Station. The data from the simultaneous measurements show that the spatial distributions of NLC and PMSE in the HF band were collocated with each other, which suggests that oblique sounding HF radar is a useful tool for estimating the 2-D horizontal distribution of PMSE.

2. Observations

During a 1.5 h interval from 2000 to 2130 UT (2300 to 0030 LT; LT=UT+3 hours) on Feb. 11, 2009, NLC were observed at Syowa Station using a high-resolution digital camera (Nikon D3) with a 70 mm lens at f/4, shutter speed of 1/15 s, and ISO of 200. Figure 1a shows a photograph of the NLC taken at Syowa Station at around 2033 UT on Feb. 11, 2009. NLC can be seen as faint, wavy, and bluish-white structures above the top of the hill. This picture was taken when the sun was well below the horizon, but still illuminating the NLC at mesospheric altitudes. Figure 1b shows a processed image of Fig. 1a (the original image was first converted to a monochromatic image and then the spatially averaged intensity was subtracted from the monochromatic image to enhance the visibility of the NLC structures), in which many small-scale traces due to gravity waves embedded within the NLC are more pronounced. The field-of-view (FOV) of the camera was directed toward the southwest (the direction of geographic south is marked with the dashed line in the easternmost part of the FOV); thus the NLC were located roughly south of Syowa Station. At this time, NLC appeared only in the middle of the FOV, as marked with a white square in Fig. 1b. Hereafter we refer to this region of NLC as NLC-A to aid discussion. Figures 2a and 2b show the original and processed images of NLC, respectively, both of which were taken at 2100 UT. Until this time, NLC-A had clearly moved westward, which suggests that the direction of the background neutral wind was predominantly westward during this time. A movie of the NLC photographs confirmed this westward movement (not shown). More importantly, another region of NLC can be identified in the upper part of the FOV, as marked with a black square in Fig. 2b (hereafter we refer to this region as NLC-B). The signature of small-scale structures within NLC-B was less clear than in NLC-A. At the time of the first image (Fig. 1), there was no evidence of wavy features in this area. Thus, NLC-B was transported from east by the westward directed background neutral wind. The FOV of the camera was 28.84° in the horizontal direction and 19.46° in the vertical direction. The elevation angle of the antenna on top of the hill was 5.10°. This information was used to map the NLC region with a geographic coordinate system. Note that the geographic location of NLC-B was closer to Syowa Station, if we assume that both of the NLC in these two

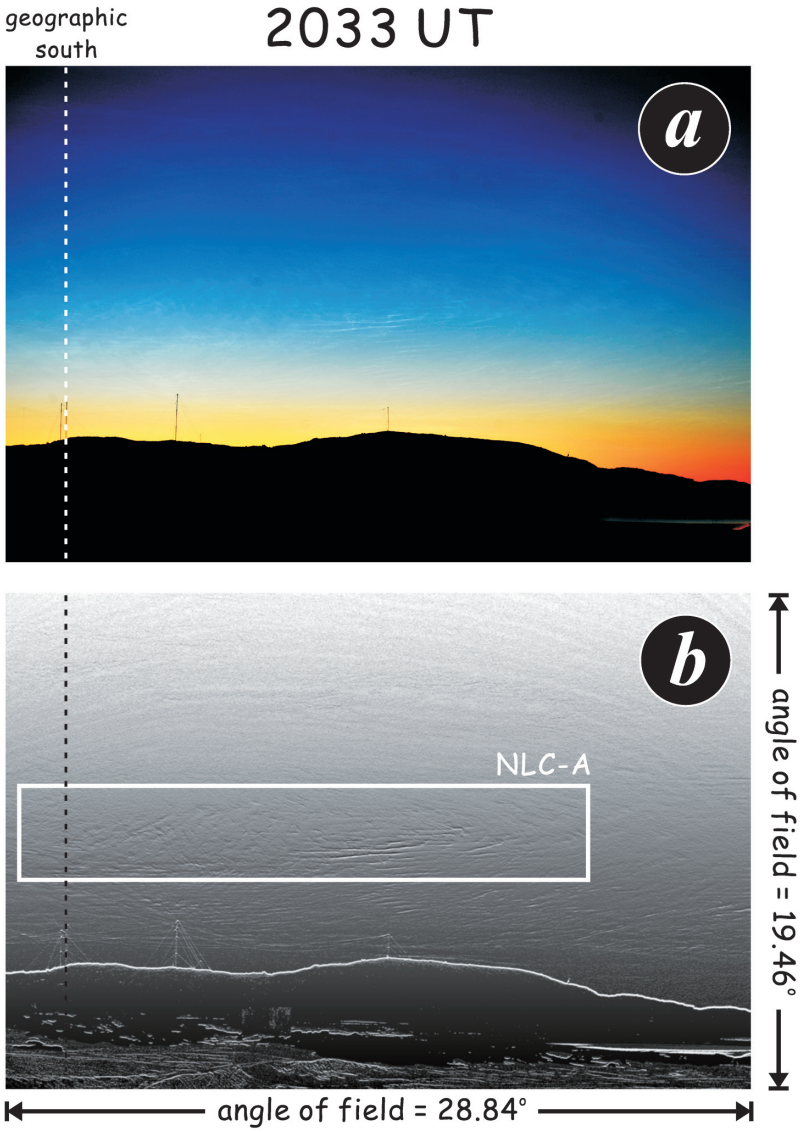

Fig. 1. (a) Photograph of NLC taken at Syowa Station at 2033 UT on Feb. 11, 2009. The field-of-view of the camera is directed roughly toward the geographic south; (b) processed image of the photograph in the upper panel.

regions were located at the typical NLC altitude around 84 km (Klekociuk *et al.*, 2008; Taylor *et al.*, 2009).

Throughout the interval during which NLC were observed at Syowa Station, the two coherent HF radars of Syowa-South & East HF radars of NIPR for SuperDARN (SENSU), which form part of the international network of coherent HF radar known as the Super Dual Auroral Radar Network (SuperDARN, Greenwald *et al.*, 1995; Chisham *et al.*, 2007), were operative. Figure 3 depicts the FOV of the Syowa South and Syowa East radars of SENSU

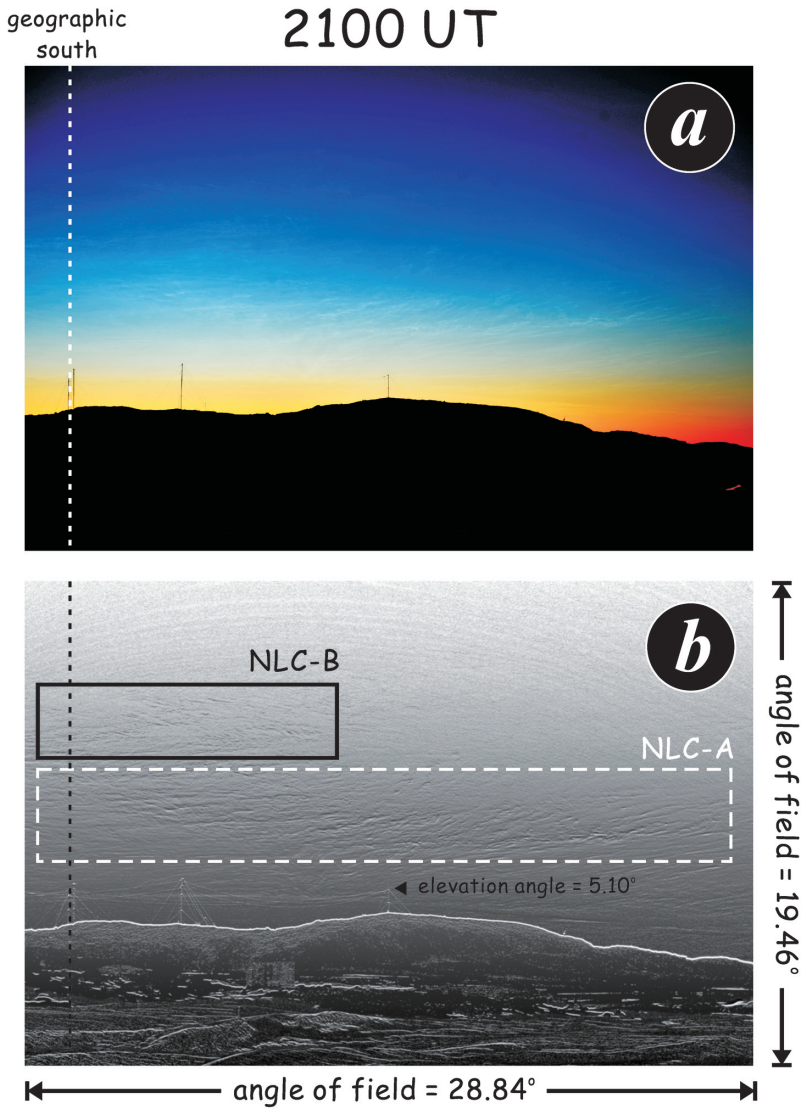

Fig. 2. (a) Photograph of NLC taken at Syowa Station at 2100 UT on Feb. 11, 2009; (b) processed image of the photograph in the upper panel.

mapped on the geographic coordinate system. The radar beam in normal operational mode is sequentially scanned through 16 directions with a step in azimuth of 3.33°. It takes approximately 3 s to integrate backscatter returns in one beam direction and about 60 s is needed to perform a scan of all directions. During the interval of interest, the first range gate was set to 180 km for Syowa East and 270 km for Syowa South, with a range resolution of 45 km. The operating frequency was around 12.5 MHz for Syowa South and 10.4 MHz for Syowa East. In each radar cell, routine analysis of the auto-correlation functions obtained provides the backscatter power, spectral width, and the Doppler shift of the echo spectra.

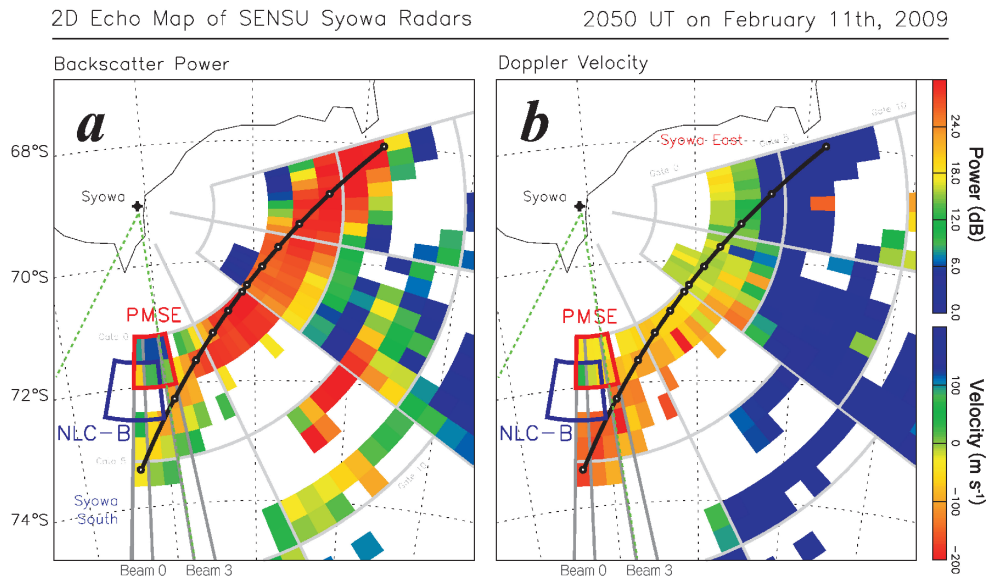

*Fig. 3. The fields-of-view of the Syowa South and Syowa East radars of SENSU in a geographic coordinate system, where (a) the backscatter power and (b) the Doppler velocity at 2050 UT are superimposed. The black thick line with open circles indicates locations where the angles between the radar wave and the local geomagnetic field vectors are close to 90° (*i.e.*, the normality condition is satisfied).*

In Fig. 3a, the 2-D spatial distribution of the backscatter power at 2050 UT is superimposed on the FOV of the two radars. The SuperDARN radars were originally designed to observe coherent echoes from field-aligned irregularities (FAIs) in the E- and F-regions of the ionosphere. FAIs in the E-region are known to be most prominent in the ranges close to the radar site (*e.g.*, closer than 600 km in slant range). For this reason, we assumed that the SuperDARN backscatters in Fig. 3a originated from the E-region at a height of 100 km when we mapped the echoes onto the geographic coordinate system. Because PMSE detected with the SuperDARN radar also appear at these range gates (Ogawa *et al.*, 2002), it is crucial to distinguish PMSE from E-region FAIs correctly. One possible way to remove E-region FAIs is to predict the spatial distribution of E-region backscatters by examining the angle between the radar wave vector and the local geomagnetic field. Past studies of E-region echoes in the HF band (*e.g.*, Milan and Lester, 2001) indicated that coherent radar echoes from E-region FAIs are most strongly backscattered when the angles between the radar wave and the local geomagnetic field vectors (A) are close to 90° (*i.e.*, the perpendicularity condition is satisfied) and form an L-shell aligned structure. Koustov *et al.* (2001) demonstrated that strong E-region echoes in the Syowa radars are expected to be obtained from slant ranges of 250–320 km on beam 15 (beam 0) of Syowa South (Syowa East), while on beam 0 (beam 15) of Syowa South (Syowa East) they are obtained from slant ranges of 400–500 km. The black thick line in Fig. 3 indicates locations where the perpendicularity condition is satisfied at an altitude of 110 km. This line of perfect perpendicularity is consistent with the distribution of E-region

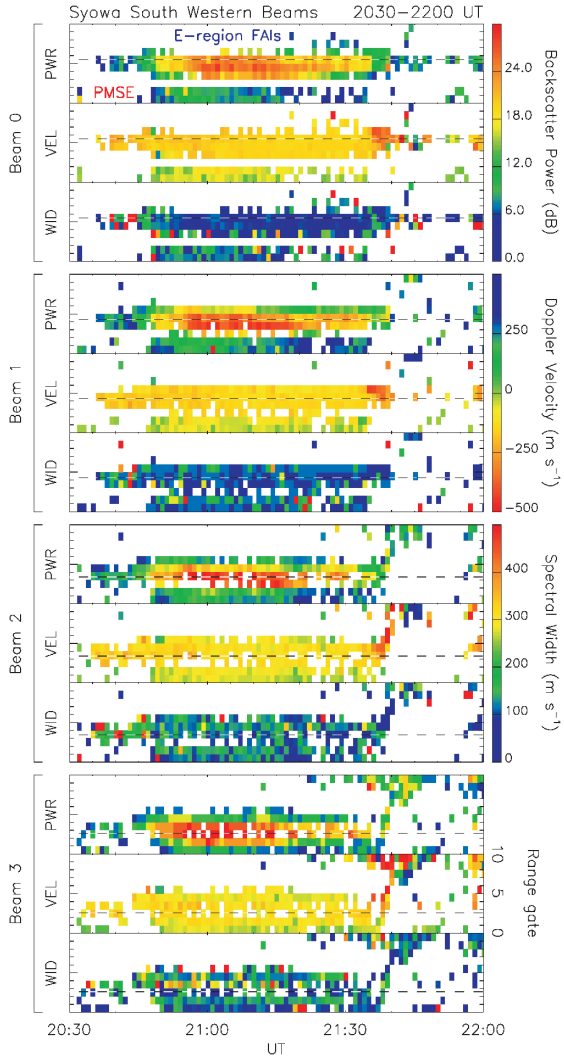

Fig. 4. Radar data from the four westernmost beams (beam 0–3) of Syowa South during 2030–2200 UT, in which the backscatter power, Doppler velocity, and spectral width are plotted in the RTI format. The horizontal dashed lines indicate lines of perfect perpendicularity.

echoes shown by Koustov *et al.* (2001); thus it gives a nominal location of the E-region backscatters in the Syowa radar observations.

The 2-D distribution of the backscatter power shown in Fig. 3a indicates that a band of strong radar backscatter appeared to follow the line of perfect perpendicularity. These strong echoes were produced from closer ranges on beam 15 (beam 0) of Syowa South (Syowa East), while on beam 0 (beam 15) of Syowa South (Syowa East) they were produced from distant ranges. This strongly suggests that the band of strong radar backscatter seen in Fig.

3a was associated with FAIs in the E-region altitudes. In Fig. 3b, the Doppler velocity data are superimposed on the FOV of the two Syowa radars. The maximum amplitude of the Doppler velocity within the band of E-region backscatter was as large as 200 m s^{-1}. The spectral widths were also greater than 100 m s^{-1} (not shown in Fig. 3, but the spectral width data from the westernmost three beams are shown in Fig. 4). These values were clearly larger than those of typical PMSE in the SuperDARN data (Hosokawa *et al.*, 2005). In addition, the velocity was "away from the radar" along the western beams of Syowa South and "toward the radar" along the eastern beams of Syowa East. This systematic change in the line-of-sight Doppler velocity is consistent with sunward ionospheric convection in this local time sector (~21 MLT), which also indicates that the band of strong echoes in Fig. 3a originated from FAIs in the E-region altitudes. During 1800–2200 UT, a small perturbation was observed in the magnetogram at Syowa Station (~30 nT), which implies that weak auroral activities occurred in the region. The band of E-region echoes was possibly associated with such auroral activities.

The origin of the band of strong radar echoes in Fig. 3a was not PMSE in the mesosphere but FAIs in the E-region of the ionosphere; thus the echoes had no direct relationship with the NLC observed from Syowa Station. However, further examinations of the backscatter power data along the westernmost four beams (beam 0 to 3) of Syowa South revealed slightly weaker echoes at the closest two range gates (gate 0 and 1), which are marked with red squares in Fig. 3. The spatial structure of this echo region was clearly distinct from the band of strong E-region echoes. In addition, the parameters observed in this region were quite different from those of the E-region echoes. For example, the Doppler velocity was very small (less than 100 m s^{-1}) and the spectral width was extremely narrow (less than 50 m s^{-1}) (not shown). These radar parameters were consistent with those of PMSE in the HF band reported by Ogawa *et al.* (2002, 2003), which allows us to regard these near-range echoes as possible signatures of PMSE in the HF band. The backscatter power of this echo region was mostly less than 10 dB, which was much weaker than the E-region echoes. In these beam directions, however, the E-region echoes were observed at relatively distant range gates (gate 3 to 5). Hence, these weak echoes at the closest ranges could be observed without being masked by the stronger E-region FAIs.

Figure 4 shows the radar data from the four westernmost beams (beam 0 to 3) of Syowa South during 2030–2200 UT, in which the backscatter power (PWR), Doppler velocity (VEL), and spectral width (WID) are plotted in the Range-Time-Intensity (RTI) format. These beams were facing almost toward the geographic south, in which direction the photographs of NLC shown in Figs. 1 and 2 were taken. The horizontal dashed line indicates the location of perfect perpendicularity for each beam direction. If the data from beam 0 (top three panels) are considered, it can be seen that echoes with a strong backscatter power were observed at range gates from 3 to 6. The location of these strong echoes followed the line of perpendicularity in all the beam directions shown in Fig. 4, which again suggests that these echoes originated from FAIs in E-region altitudes. In the closest two range gates along beam 0, relatively weaker echoes appeared at around 2045 UT, clearly apart from the E-region backscatters, and they continued for approximately 1 h. These are the echoes marked with red squares in the 2-D maps shown in Fig. 3. The backscatter power of this echo region was clearly weaker (less than 10 dB) than that of the E-region backscatters. The Doppler velocity was mostly less than 100 m s^{-1}, which is also clearly less than that of the E-region echoes.

This considerable difference again indicates that these echoes in the closest two range gates were not associated with FAIs in the ionosphere but were a possible signature of PMSE in the HF band. This signature can be seen along all the beams in Fig. 4. However, the echoes tended to become hidden behind the E-region echoes with increasing beam number (from beam 0 to beam 3) because the stronger E-region echoes moved closer to the radar site and masked the weaker echoes at the closest ranges. As a result, the possible PMSE signatures were visible only along the westernmost beams of Syowa South.

3. Discussion and Summary

We observed HF echoes in range gates very close to the radar site, whose characteristics were consistent with those of PMSE in the SuperDARN data (Ogawa *et al.*, 2002, 2003; Hosokawa *et al.*, 2005), during an NLC event on Feb. 11, 2009. The possible sources of such near range echoes are sporadic-E layer (Es) or PMSE (Ogawa *et al.*, 2002). However, an FMCW ionospheric sounder at Syowa Station, which provides ionograms every 2 min, observed no Es signature throughout the interval of interest; thus the source of the echoes is likely to be PMSE at mesospheric heights. In Fig. 2, we introduced two regions of NLC: NLC-A and NLC-B. We estimated the geographic locations of these NLC regions assuming the height of the layer was 84 km (based on Lidar observations in the SH by Klekociuk *et al.*, 2008). Because NLC-A was located farther away from the radar site, only the spatial distribution of NLC-B is shown (with blue squares) in Fig. 3. Here, we also show the FOV of the digital camera in the longitudinal direction by the dashed green lines. A small displacement was apparent between the locations of possible PMSE echoes (red square) and NLC-B (blue square). However, if we take the poor spatial resolution of the SuperDARN measurement (45 km) into account, the spatial collocation between these two features was good. This agreement between visible NLC and the near-range echoes again supports the assumption that the peculiar near range echoes reported by Ogawa *et al.* (2002) actually correspond to a PMSE signature at the HF band. However, it should be noted that different heights were assumed in Fig. 3 for mapping the SuperDARN echoes (100 km) and NLC-B (84 km). When the SuperDARN backscatters were mapped using the 84 km height assumption, the location of the echoes was close to the Syowa Station. This clearly affects the suggested spatial collocation between the SuperDARN near-range echoes and NLC-B. The other important point to note is that some of the SuperDARN radars have an offset in the range determination. For example, Tsutsumi *et al.* (2009) showed that one of the SuperDARN radars in Scandinavia (CUTLASS Finland) has an offset of 50 km in the determination of range. Such an offset could also affect the comparison made in the present study. For a more rigorous comparison, the range determination of the two SuperDARN radars in the Syowa Station must be calibrated.

As shown in Fig. 4, the near-range echoes in the westernmost beams of Syowa South appeared at around 2045 UT and continued until around 2135 UT. NLC were observed throughout the 1.5 h interval from 2000 to 2130 UT. The timings of the first observations of the NLC and the echoes differed from each other (the duration of the NLC observations was longer by 45 min), although the end times were similar. However, as mentioned above, the PMSE in the SuperDARN data appeared only in the region of NLC-B (*i.e.*, the radar could not sense the PMSE associated with NLC-A). NLC-B were not observed in the first half of

the time period when NLC were observed (NLC-B was first observed at around 2055 UT). This explains the discrepancy in the start times of NLC and PMSE.

The most important conclusion from these measurements is that the oblique sounding HF radars such as those used in SuperDARN are useful for estimating the spatial distribution of PMSE. The PMSE here were identified along the southward looking beams (beams 0–3) of the Syowa South radar, only when NLC appeared in the ranges very close to the radar site. Unfortunately, E-region FAIs masked the PMSE in other beam directions; thus we could not estimate the full distribution of PMSE using data from all beam directions. However, if NLC appeared during an interval with no E-region echoes, we could visualize the horizontal structure of PMSE, especially in the longitudinal direction. Such 2-D observations of PMSE were recently reported by Taylor *et al*. (2009), who used incoherent scatter radar at Poker Flat, Alaska, USA, to observe the 2-D structure of PMSE during a period of NLC. Their data clearly showed that the spatial structure of PMSE is far from uniform and contains various mesoscale structures. Such a localized structure of NLC and PMSE is probably associated with a small-scale structure in the wind, which possibly controls the advection of cold air and/or the transportation of ice particles producing NLC/PMSE. Morris *et al.* (2007) demonstrated the relationship between the occurrence of PMSE and the equatorward wind above Davis Station in Antarctica. They suggested that both local and global effects control the mesospheric temperature over Davis Station. The zonal-mean meridional wind (zonally averaged flow in the meridional direction) driven by the action of gravity waves adiabatically cools the polar mesosphere and local wind flowing equatorward transports cold air from the poles, both of which can chill the mesosphere and result in the appearance of NLC/PMSE. Morris *et al.* (2007) related daily averaged wind data to the occurrence of PMSE; thus the possible effects of small-scale temporal and spatial variations of wind on the transient appearance of PMSE are still unclear. During the current observations, NLC-B were first noticed in the FOV of the SuperDARN during a westward neutral wind and PMSE were subsequently observed by the radar. This highlights the importance of investigating the localized appearance of PMSE in relation to the horizontal transportation of NLC with the background neutral wind. Unfortunately, the Syowa South radar observed PMSE only along the four westernmost beams; thus, it was impossible to determine the neutral wind perpendicular to the beam direction (*i.e.*, the east-west direction during these observations) using the beam-swinging technique. However, in future research, the motion of NLC from optical data and the neutral wind derived from SuperDARN will be systematically compared.

In further research, we intend to extend this study by making 2-D observations of NLC, PMSE, and the background wind. We will continue to study simultaneous observations of NLC/PMSE using optics and SuperDARN over Syowa Station. However, the spatial resolution of the SuperDARN radars may be too coarse to resolve the fine scale structure of PMSE. A huge MST radar will shortly be operative at the Syowa Station (Program of the Antarctic Syowa MST/IS Radar: PANSY), which will allow us to visualize the distribution of PMSE near Syowa Station with improved spatial and temporal resolution. In addition, Rayleigh-Raman Lidar has been operative at the Syowa Station since 2010 and can also be used for observing NLC as a form of Polar Mesospheric Clouds (PMC). By combining these new measurements at the Syowa Station with the existing SuperDARN radar system, it will be possible to resolve questions such as "what kind of factors control

the localized distribution of NLC/PMSE?"

Acknowledgements

The Syowa HF radar system is supported by the Ministry of Education, Culture, Sports, Science and Technology of Japan. The radar and digital camera were operated as a part of the 50th Japanese Antarctic Research Expedition (JARE-50) projects.

References

Chisham, G. *et al.* (2007): A decade of the Super Dual Auroral Radar Network (SuperDARN): scientific achievements, new techniques and future directions. Surv. Geophys., **28**, 33–109, doi: 10.1007/s10712–007–9017–8.

Cho, J.Y.N. and Röttger, J. (1997): An updated review of polar mesosphere summer echoes: Observation, theory, and their relationship to noctilucent clouds and subvisible aerosols. J. Geophys. Res., **102**, 2001–2020, doi: 10.1029/96JD02030.

Greenwald, R.A. *et al.* (1995): DARN/SuperDARN: A global view of the dynamics of high-latitude convection. Space Sci. Rev., **71**, 761–796, doi: 10.1007/BF00751350.

Hosokawa, K., Ogawa, T., Yukimatu, A.S., Sato, N. and Iyemori, T. (2004): Statistics of Antarctic mesospheric echoes observed with the SuperDARN Syowa Radar. Geophys. Res. Lett., **31**, L02106, doi: 10.1029/2003GL018776.

Hosokawa, K., Ogawa, T., Arnold, N.F., Lester, M., Sato N. and Yukimatu A.S. (2005): Extraction of polar mesosphere summer echoes from SuperDARN data. Geophys. Res. Lett., **32**, L12801, doi: 10.1029/2005GL022788.

Klekociuk, A.R., Morris, R.J. and Innis, J.L. (2008): First Southern Hemisphere common-volume measurements of PMC and PMSE. Geophys. Res. Lett., **35**, L24804, doi: 10.1029/2008GL035988.

Koustov, A.V., Igarashi, K., André, D., Ohtaka, K., Sato, N., Yamagishi, H. and Yukimatu, A. (2001): Observations of 50- and 12-MHz auroral coherent echoes at the Antarctic Syowa station. J. Geophys. Res., **106**, 12875–12887, doi: 10.1029/2000JA000165.

Latteck, R., Singer, W., Morris, R.J., Holdsworth, D.A. and Murphy, D.J. (2007): Observation of polar mesosphere summer echoes with calibrated VHF radars at 69° in the Northern and Southern hemispheres. Geophys. Res. Lett., **34**, L14805, doi: 10.1029/2007GL030032.

Lübken, F.-J. and von Zahn, U. (1991): Thermal structure of the mesopause region at polar latitudes. J. Geophys. Res., **96**, 20841–20857, doi: 10.1029/91JD02018.

Lübken, F.-J., Müllemann, A. and Jarvis, M.J. (2004): Temperatures and horizontal winds in the Antarctic summer mesosphere. J. Geophys. Res., **109**, D24112, doi: 10.1029/2004JD005133.

McIntyre, M.E. (1989): On dynamics and transport near the polar mesopause in summer. J. Geophys. Res., **94**, 14617–14628, doi: 10.1029/JD094iD12p14617.

Milan, S.E. and Lester, M. (2001): A classification of spectral populations observed in HF radar backscatter from the E region auroral electrojets. Ann. Geophys., **19**, 189–204, doi: 10.5194/angeo-19–189–2001.

Morris, R.J., Murphy, D.J., Reid, I.M., Holdsworth, D.A. and Vincent, R.A. (2004): First polar mesosphere summer echoes observed at Davis, Antarctica (68.6°S). Geophys. Res. Lett., **31**, L16111, doi: 10.1029/2004GL020352.

Morris, R.J., Murphy, D.J., Klekociuk, A.R. and Holdsworth, D.A. (2007): First complete season of PMSE observations above Davis, Antarctica, and their relation to winds and temperatures. Geophys. Res. Lett., **34**, L05805, doi: 10.1029/2006GL028641.

Nussbaumer, V., Fricke, K.H., Langer, M., Singer, W. and von Zahn, U. (1996): First simultaneous and common volume observations of noctilucent clouds and polar mesosphere summer echoes by lidar and radar. J. Geophys. Res., **101**, 19161–19167, doi: 10.1029/96JD01213.

Ogawa, T., Nishitani, N., Sato, N., Yamagishi, H. and Yukimatu A.S. (2002): Upper mesosphere summer echoes detected with the Antarctic Syowa HF radar. Geophys. Res. Lett., **29**(7), 61, doi: 10.1029/2001GL014094.

Ogawa, T., Arnold, N.F., Kirkwood, S., Nishitani, N. and Lester, M. (2003): Finland HF and Esrange MST radar observations of polar mesosphere summer echoes. Ann. Geophys., **21**, 1047–1055, doi: 10.5194/angeo-21–1047–2003.

Rapp, M. and Lübken, F.-J. (2004): Polar mesosphere summer echoes (PMSE): Review of observations and

current understanding. Atmos. Chem. Phys., **4**, 2601–2633, doi: 10.5194/acp-4–2601–2004.
Taylor, M.J. *et al.* (2009): Coordinated optical and radar image measurements of noctilucent clouds and polar mesospheric summer echoes. J. Atmos. Sol.-Terr. Phy., **71**, 675–687, doi: 10.1016/j.jastp.2008.12.005.
Tsutsumi, M., Yukimatu, A.S., Holdsworth, D.A. and Lester, M. (2009): Advanced SuperDARN meteor wind observations based on raw time series analysis technique. Radio Sci., **44**, RS2006, doi: 10.1029/2008RS003994.
Woodman, R.F., Balsley, B.B., Aquino, F., Flores, L., Vazquez, E., Sarango, M., Huaman, M.M. and Soldi, H. (1999): First observations of polar mesosphere summer echoes in Antarctica. J. Geophys. Res., **104**, 22577–22590, doi: 10.1029/1999JA900226.